APPLIED MICROBIOLOGY
Vol. 12, No. 1, p. 37–43 January, 1964

Calibration of a Modified Andersen Bacterial Aerosol Sampler

K. R. MAY[1]

Fort Detrick, Frederick, Maryland

Received for publication 5 September 1963

ABSTRACT

MAY, K. R. (Fort Detrick, Frederick, Md.). Calibration of a modified Andersen bacterial aerosol sampler. Appl. Microbiol. **12**:37–43. 1964.—A study of the flow regime in the commercial Andersen sampler revealed defects in the sampling of the larger airborne particles. Satisfactory sampling was obtained by redesigning the hole pattern of the top stages and adding one more stage to extend the range of the instrument. A new, rational hole pattern is suggested for the lower stages. With both patterns a special colony-counting mask can be used to facilitate the assay. A calibration of the modified system is presented which enables particle size distribution curves to be drawn from the colony counts.

The Andersen (1958) sampler collects six size-graded aerosol fractions in petri dishes by a system of multi-jet cascade impaction. It has found wide acceptance for sampling viable aerosols when it is desired to estimate the numbers and sizes of the actual airborne particles, rather than the total number of viable cells in those particles, as yielded by liquid impingers.

I wished to make a particle-size calibration of the commercial sampler (model 0101), so that size-distribution curves of the sampled cloud could be obtained either from colony counts or mass of material per stage. It is essential for such work that all jets in each stage should impact equally. It was found that, while the lower stages were adequate in this respect, stages 1 and 2 always showed large differences in impaction performance in different areas of a stage, making a valid calibration impossible. The intake efficiency for the larger particles was also poor. This paper reports a study of these faults, which enabled a modified design to be developed and calibrated.

In justification for the improvement to the large (>5 μ in diameter) particle efficiency of this sampler, it is pointed out that in this category fall many of the infective particles generated by such processes as blanket shaking, sweeping, talking, coughing, and sneezing. Also, a high proportion of the mass of sprayed aerosols usually lies in the larger particles.

MATERIALS AND METHODS

Preliminary studies. Glass discs were set up in the special petri dishes at exactly the same height as is the agar with the standard fill of 27 ml. This setting is very important because the clearance between the underside of the sieve plate (S in Fig. 1) and the collection surface affects the airflow. Andersen (1958) gave this clearance as 0.1 in., but our measurements gave 0.07 to 0.095 in., varying with the dish used, the age of the agar, and the posture of the sampler. The average thickness of agar is 0.175 in.

Heavy samples from dyed liquid aerosols were then taken. Each impact spot on a disc was then the aggregate of many droplets, and its density relative to its fellows indicated the uniformity or otherwise of jet efficiency over a stage. Samples of viable particles of sprayed *Serratia marcescens* were also studied.

Modified sampler. Uniform efficiency over a stage was obtained by a complete redesign of the jet hole pattern and jet-to-agar clearances. It was strongly desired to extend the useful range of the sampler to particles larger than 12 μ. This was done by adding a top stage of the same new design, after tests with other geometry, including a single-jet stage.

Intake efficiency and internal losses. Studies were made of the efficiency of collection of particles up to 30 μ, by taking samples, in a large chamber, of dyed, involatile, and uniform droplets generated by a spinning-top sprayer. Colorimetric estimations were made of the dye washed from the glass discs and from other parts of the sampler. It has not been possible, to date, to study the important question of intake efficiency in windborne aerosols.

Calibration. A review of the calibration of cascade impactors has been given by Mercer (1963). He prefers the use of the "50% cut-off" diameter (d_{50}) as a stage characteristic rather than the mass median diameter (MMD). At a standard sampling rate, the former cannot vary whereas it is possible for the MMD to show some variation with atypical aerosol distributions. In the present work, values for both d_{50} and MMD were obtained.

Calibration was done by detailed fluorescent-microscope counting and sizing of bacterial aerosol particles sampled on sticky discs. The eyepiece graticule described by May (1945) was used in this work, and two observers gave very consistent results. At least 300 particles were sized per stage in each experiment, and enough impact areas were completely scanned to give a count of at least 3,000 particles per stage and thus a reliable estimate of the total stage numbers.

[1] Present address: Microbiological Research Establishment, Porton, Wiltshire, England.

Pneumatic spraying of suspensions at 2×10^{11}/ml of *Aerobacter aerogenes* produced the test particles. The suspensions had been heat-sterilized, stained with primuline dye, centrifuged, and resuspended in clean water. The resulting particles after evaporation of the water are inert, strongly fluorescent under ultraviolet light, and spherical, except for the smallest particles, which consist of single, or very few, cells with a density of 1.37 g/cm^3. This is similar to the density of most other bacterial particles. The fluorescent particles are very easy to see, cannot be confused with atmospheric dust, and have realistic physical properties. Wax spheres made by spraying hot molten wax, as widely used in similar work (e.g., Andersen, 1958), were not used here because it was found by flotation methods that variable included air bubbles gave them a wide range of density. Also, doublet spheres were common.

From the size counts of each stage, the best fit cumulative number distribution curves were plotted on log-probability paper. In general, these curves gave very good straight lines over most of their length. From these, smoothed frequency histograms of absolute numbers of particles sampled per size range were drawn for each stage. The intersections of these are the d_{50} values. The same curves also yielded the characteristic cut-off curves for each stage (Fig. 9). MMD values were obtained from conventional plots of the cumulative volume on log-probability paper. For each stage, the final required parameter, the mean volume diameter (MVD), is $(\sum n\, d^3/\sum n)^{1/3}$ where there are n particles in each range of mean diameter d.

RESULTS

Figure 2 is a photograph of a heavy sample of dyed droplets on the first three Andersen stages. The maximal drop diameter was 12 μ. Note that there are severe density variations over the stage 1 discs, both with and without the intake cone, and on stage 2. On stage 3 it is just detectable in the original that the spots slightly increase in density from inside outwards. Stages 4, 5, and 6 are not shown because they appear quite uniform.

These effects were found to arise from interactions of factors which may be called (i) radial pressure fall (rpf), (ii) pattern interference, (iii) particle size, and (iv) intake cone. Table 1 gives data on the static pressures Px, Py, and Pz in zones X, Y, and Z.

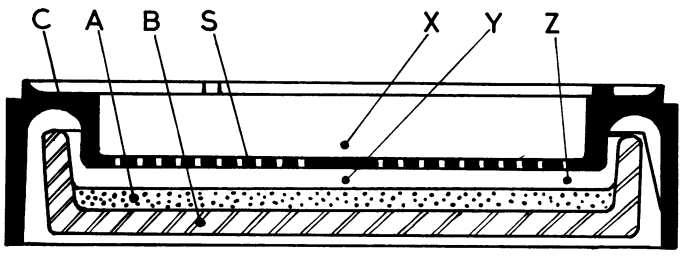

FIG. 1. *Vertical section through an Andersen stage. A, agar in petri dish (B); C, metal body, integral with sieve plate (S), drilled with 400 holes which decrease in size from stage to stage; X, zone above S; Y, zone under center of S; Z, zone under outer ring of holes.*

(i) There is no flow in zone Y but the full 1 ft^3/min flows through zone Z. Therefore, from Bernoulli's theorem Pz < Py, so that there is always more flow through the outer jets than the inner ones. The magnitude of rpf, Py − Pz, relative to the pressure fall across the jets, Px − Py, Px − Pz, determines the ratio of flow rates between the outer and inner holes. In stages 1 and 2, where rpf is comparable with jet pressure fall, there are large differences between the inner and outer jet flows (Table 1). At stage 1, twice as many particles flow through the outer holes as the inner ones and at higher impaction efficiency so that enormous differences in numbers (and size) of particles collected between inner and outer zones can occur (Fig. 2a).

By stage 3 and below, pressure fall across the smaller holes is great enough to make rpf relatively negligible, and all holes have nearly the same impaction efficiency (Fig. 2d).

The magnitude of rpf and its effects is inversely related to the distance between the jets and the impaction surface.

(ii) In Fig. 2, all samples are arranged with the hole pattern in the same orientation to show that, although it has no symmetry, the pattern does have certain recognizable hole groupings, such as the parallel "streets" of holes at 12, 2, 4, 7, and 10 o'clock. In intermediate positions, holes fall into a diamond pattern and here the relatively broad and feeble air-jets of the first two stages are readily blown outwards and fail to impact fully. The effect varies between a selective winnowing out of the smaller particles to a complete absence of particles in broad areas, as in Fig. 2c. In the "streets", jets can impact in the protective lee of those upstream so that their deposits are relatively heavy and, in combination with rpf effects, give characteristic and reproducible patterns (Fig. 2b, c).

In the lower stages the finer jets have sufficient force to overcome pattern interference.

(iii) Differences in spot density on the top stage are dependent upon particle size, because very large particles have sufficient inertia to overcome the winnowing effect of pattern interference and impaction efficiency differences of rpf. This is shown by comparing Fig. 2a, where the maximal drop size was 12 μ, with Fig. 6a, a sample taken in identical conditions except that a 20-μ uniform droplet aerosol was used.

(iv) The Andersen sampler is fitted with a cone over the top stage like an inverted funnel, with an intake hole of 1 in. diameter. This cone does not spread the aerosol evenly over the top sieve, as perhaps intended, but directs a broad jet of air at the central zone of the sieve. This impacts many large particles on the upper surface of the sieve, and those which get through the holes are preferentially impacted in the centre of the dish. Figure 6b

demonstrates this effect in the 20-μ aerosol and should be compared with Fig. 6a, its parallel sample with no cone. Quantitative estimation of these samples showed that of the drops entering the cone, in Fig. 6b, 87% were lost on the sieve and 13% were recovered from the dish, whereas 78% was recovered from the dish in Fig. 6a. These effects increase with the particle size, but even with droplets of 12 μ and below the cone effect is very obvious, as seen by comparing the two parallel stage 1 samples in Fig. 2a and b.

Colony patterns. Colonies from a viable aerosol of particle size distribution similar to Fig. 2 are shown in Fig. 3. Colony samples must not have an average of more than about three particles per hole, or dishes become overloaded.

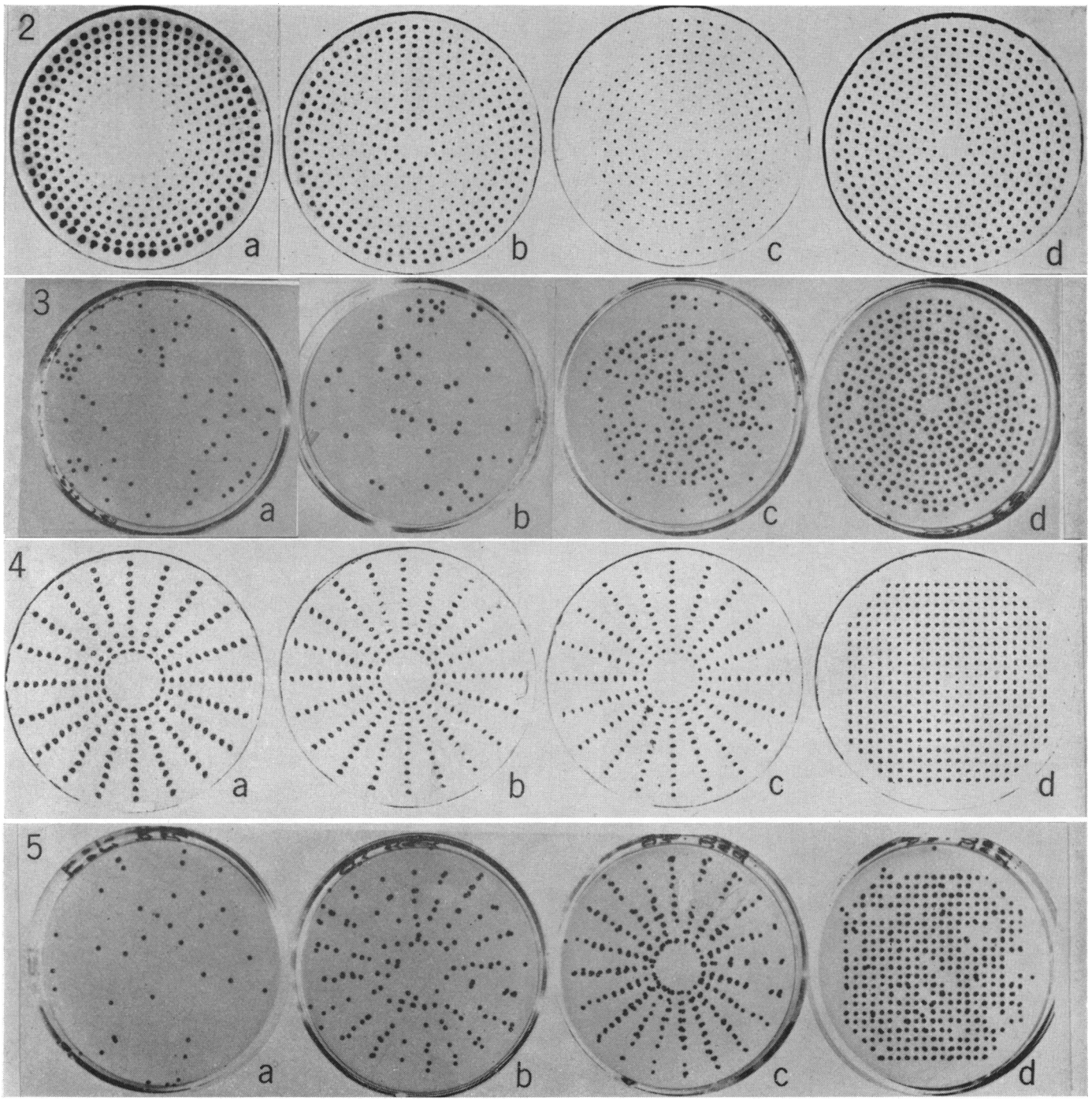

FIG. 2. *Heavy sample of dyed droplets in standard Andersen sampler. a, stage 1 without cone; b, stage 1 with cone; c, stage 2; d, stage 3.*
FIG. 3. *Colonies of Serratia marcescens from standard Andersen sampler; a, b, c, and d as for Fig. 2.*
FIG. 4. *Heavy sample of dyed droplets on modified stages; parallel with Fig. 2; a, stage 0; b, stage 1M; c, stage 2M; d, stage 3M.*
FIG. 5. *Colonies of Serratia marcescens from modified stages. Parallel sample with Fig. 3; a, b, c, and d as for Fig. 4.*

At this level the Poissonian statistics of the probability of a hole being occupied blur the effects of the above factors. Also, an occupied hole grows a single colony which has the same apparent "spot density" whether it grows from a single-cell particle, a particle containing thousands of cells, or from several mixed particles impacted under the same spot. Nevertheless, pattern effects can always be detected on colony samples of suitable level. Comparing the samples in Fig. 2a and 3a, we see that both "no cone" samples have a bare area in the central zone. The next colony sample, Fig. 3b, shows a heavier central zone growth than Fig. 3a, induced by the cone, and the growth under the outer holes shows the beginnings of preferential "street" deposition which is often obvious on this stage with heavier samples. Figure 3c is strikingly similar to Fig. 2c. Stages 3 and below always give random hole occupation, which is as desired. An independently taken photograph where pattern effects may be detected is Andersen's (1958) Fig. 6, where his stage 1 sample is directly comparable with the present Fig. 3b, and stage 2 with Fig. 3c. His dishes, of course, have a random pattern orientation. There are many other confirmatory samples at hand.

TABLE 1. *Internal static pressure differences (in mm of water) in the standard Andersen sampler*

Stage	Radial pressure fall (Py − Pz)	Pressure fall across outer and inner jets		Ratio of outer and inner jet velocities $\left(\frac{Px - Pz}{Px - Py}\right)^{\frac{1}{2}}$
		Px − Pz	Px − Py	
1	0.26	0.34	0.08	2.05
2	0.33	0.76	0.43	1.33
3	0.42	1.66	1.26	1.15
4	0.45	6.2	5.7	1.05
5	0.51	33.5	33.0	1.01
6	0.63	81.5	80.9	1.004

Modifications made. The lessons of the above study were applied in designing the new radial pattern illustrated by Fig. 4a, b, and c, where the excellent spot-uniformity over each stage will be noted. In this design, almost equal velocity and impaction efficiency for every jet in a stage has been achieved by (i) adjustment of the jet-to-agar clearance, to reduce rpf, and (ii) having the jets in mutually protective straight lines with clear and expanding avenues of escape for spent air, to eliminate pattern interference. Particle size effects are not detectable because the performance of all holes is so nearly equal. No intake cone is used.

The principal measurements and static pressure readings of the three new radial stages are given in Table 2. Note the small difference between the outer and inner jet velocities shown in the last column, which should be compared with their counterparts in Table 1.

Figure 7 shows the modified radial hole components. In the foreground, stage 1M ("M" indicates that the stage is of the modified pattern) has been disassembled to indicate the method of pressing in a new sieve-plate into the standard Andersen body to obtain the jet-agar clearances of Table 2. Jet holes in the radial stages are given a 90° countersink to half their depth. Machinists' drawings are available.

Each radial stage has 200 holes. Along each of 20 radii, 10 holes are spaced, $\frac{1}{8}$ in. apart. There is not room for more holes without nullifying the design principle of these stages. Thus, we have a total of 600 holes in three top stages, compared with 800 in the two top standard Andersen stages. Fewer holes in this >5-μ particle range is no disadvantage, because in the general nature of aerosols large particles are relatively few, so that it is highly unlikely that upper stages will become overloaded before the lower.

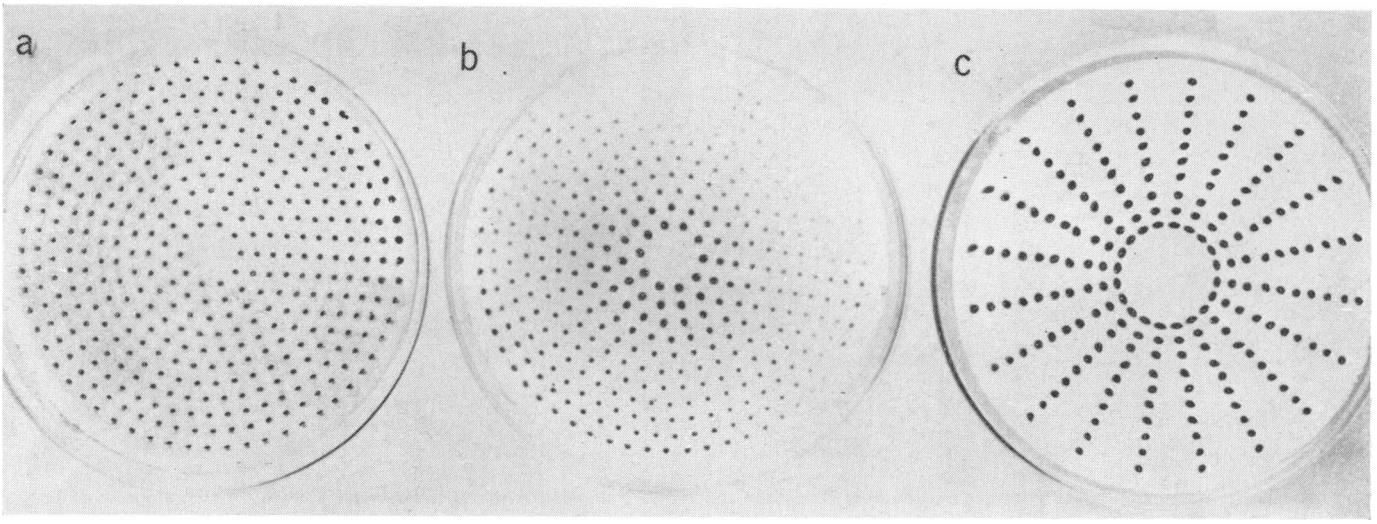

FIG. 6. *Heavy samples of dyed droplets of 20 μ diameter; a, standard Andersen sampler stage 1 without cone; b, with cone; c, new stage 0, no cone.*

Colony growth in the new stages 0, 1M, and 2M is shown in Fig. 5, and compares with Fig. 3 which is a parallel sample. Figure 5a, b, and c show 16, 109, and 182 positive holes (total 307) giving corrected counts, from the "positive hole conversion table" (Andersen, 1958) modified as described below, of 17, 157, and 482 (total 656). Figure 3b and c show 56 and 185 colonies (total 241), which become on correction 60 and 248 (total 308), though Andersen considers that the counts on his top two stages should not be corrected. In any case the new stages show a much higher count due to the improved intake and deposition of particles. The radial pattern of the very light sample (Fig. 5a) is not apparent until the counting mask, described later, is used. Figure 6 compares the intake performance of parallel samples in a 20-μ, uniform droplet cloud; Fig. 6a and b have already been quoted as yielding 78 and 13% of the probable absolute sample. Dish c (Fig. 6) yielded 85%. In a 30-μ aerosol, dishes a, b, and c yielded 47, 4, and 67%, respectively. The improvement of dish c over dish a is due entirely to having larger holes with a countersunk lead-in. This greatly reduces the particle loss, observed to occur close to the entrance of the standard parallel holes, because velocity gradients are less.

Colony counting procedure. Microscopy of the deposits of bacterial particles showed that the effective deposit area of a jet has roughly twice the diameter of the jet. On the new stage 0, the jet hole diameter is 1.85 mm, and individual colonies can therefore usually be counted if they are not larger than about 0.5 mm and are few in number. If they are larger or if there is coalescence of colonies, as in Fig. 5b and c, "positive holes" should be counted and corrected as described by Andersen (1958). Corrections for the counts from the new 200-hole stages can readily be obtained from Andersen's 400-hole table. If n positive holes are counted, the corrected number for $2n$ holes is read from the 400-hole table and that number is halved.

Some colonies are found to be out of the hole pattern. These should be ignored, on whatever stage they may be, because they are usually from small particles which have been deposited by the turbulence between jets, on their way to the stages below. The identification of in-pattern colonies on these radial stages is eased by the use of the mask shown on the left in Fig. 8. Translucent plastic is probably the best mask material. When the mask is correctly oriented in or under the petri dish, positive or negative holes are instantly recognized by looking through the holes of the mask. On heavy deposits it is quicker to count the few negative holes rather than the many positive ones. The holes are of the same size as for stage 0. The pattern of the holes is a slight expansion of the stage

TABLE 2. *Characteristics of modified, 200-hole radial pattern stages*

Stage	Hole diam	Jet-agar clearance	Py − Pz*	Px − Pz*	Px − Py*	$\left(\frac{Px - Pz}{Px - Py}\right)^{\frac{1}{2}}$
	in.	*in.*				
0	0.073	0.22	0.022	0.155	0.133	1.08
1M	0.0595	0.15	0.080	0.35	0.27	1.14
2M	0.049	0.11	0.13	0.76	0.63	1.10
3 & below	Standard	0.09		See Table 1		

* Expressed as mm of water.

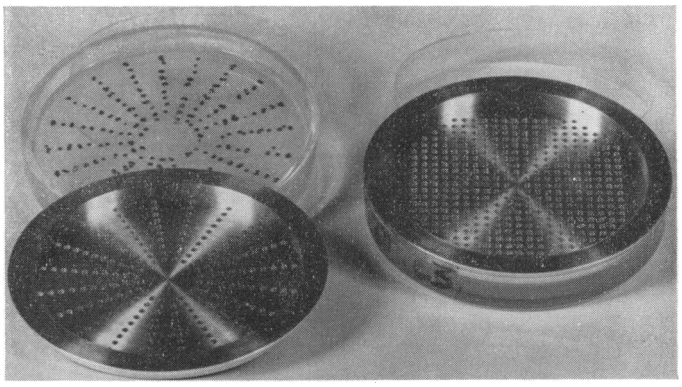

FIG. 8. *Counting masks for radial and rectangular hole patterns.*

FIG. 7. *Modified stages. Stage 1M disassembled.*

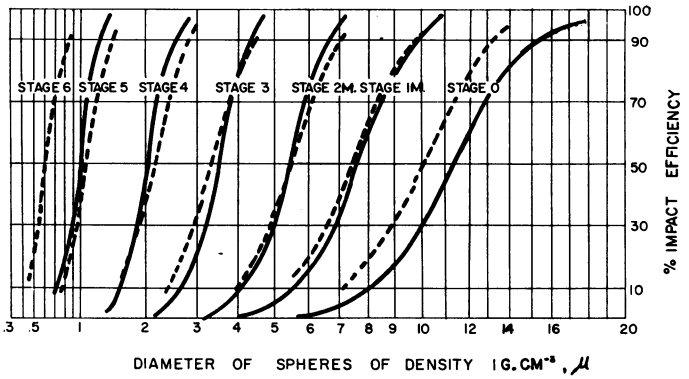

FIG. 9. *Stage cut-off curves for modified Andersen sampler. Stages 3, 4, 5, and 6 unmodified. Continuous curves, present calibration. Dashed curves calculated from Ranz and Wong (1952).*

0, 1, and 2 pattern because jets are dragged slightly outwards by the spent air. A drawing is available.

New hole pattern for the lower stages. The success of the counting mask on the radial stages suggested that it would be an advantage to use one for all stages. This cannot be done with the standard unsymmetrical Andersen pattern because there is no way of recognizing the correct orientation for a mask over the colonies. A new pattern must be symmetrical so that the correct mask position is unequivocal. To give maximal utilization of the agar surface in the lower stages, at least 400 holes are required; but, because holes should not be closer than $\frac{1}{8}$ in., a 400-hole radial pattern would give overcrowding. Also, a radial pattern is no longer necessary for the lower stages, as all jets impact nearly equally. The rectangular pattern of 400 holes with $\frac{1}{8}$-in. spacing, as shown in Fig. 4d, was therefore adopted. Hole sizes and other dimensions are exactly the same as for the standard stages 3–6. The mask is shown on the right of Fig. 8, and again it is a slight expansion of the hole pattern.

This system is very successful in giving a rapid count of positive or negative holes, whichever is the fewer, and in eliminating out-of-pattern colonies. Even without the mask, the colonies of Fig. 5d are obviously easier to count than the exact counterpart, Fig. 3d. The rectangular pattern greatly facilitates microscopic counting of inert particle deposits.

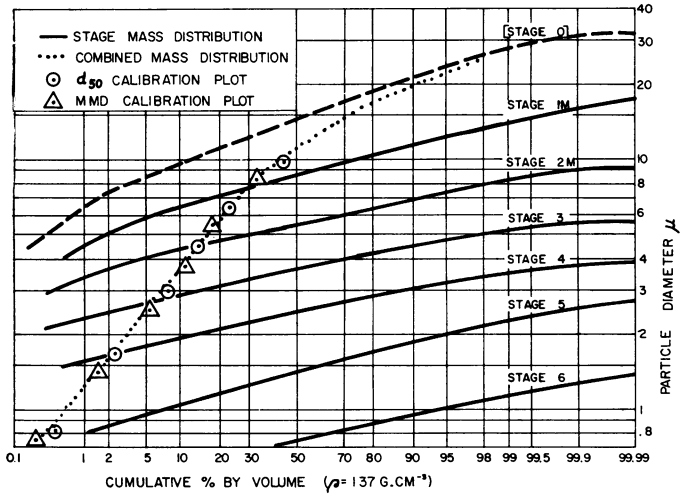

FIG. 10. *Volume distribution curves of modified Andersen sample from a sprayed bacterial aerosol.*

TABLE 3. *Calibration of modified Andersen sampler for unit density spheres and for typical bacterial particles*

Stage	At density 1 g per cm^{-3}			At density 1.37 g per cm^{-3}		
	d_{50}	Mass median diam	Mean volume diam	d_{50}	Mass median diam	Mean volume diam
	μ			μ		
0	11.2			9.5		
1M	7.5	10	8.3	6.5	8.5	7.0
2M	5.4	6.6	6.2	4.6	5.6	5.3
3	3.5	4.4	4.2	3.0	3.7	3.5
4	2.0	3.0	2.7	1.7	2.5	2.3
5	0.97	1.5	1.4	0.83	1.4	1.2
6	[0.6]*	0.9	0.85	[0.5]*	0.77	0.73

* Calculated from Ranz and Wong (1952).

Calibration. The cut-off curves for unit density spheres are shown in Fig. 9. They are strikingly similar to those calculated from the experimental results of Ranz and Wong (1952), which were obtained from a single-jet system of rather similar geometry and which are shown as dashed lines. The true curve for stage 6, which cannot be obtained from the present work, is therefore probably similar to the dashed curve for that stage.

The 0 and 1M curves have rather long "tails" due to the retention of a small number of particles down to 3 or 4 μ. This defect is inherent in the system, and could cause a spurious apparent count of large particles in aerosols having great numbers of small viable particles with very few large ones. Such error can be avoided by taking a parallel impactor sample for measurement of the largest particles by microscope, a procedure which must be done in any case to draw complete size-distribution curves.

The size range of unit density spheres on each stage, except for stage 0, can be obtained from Fig. 9. Thus, stage 3 begins to receive particles of about 4.5 μ from stage 2, and slips all particles smaller than 2.1 μ. For spherical particles of other density, ρ, all diameters should be divided by $\sqrt{\rho}$. The mass-distribution curves for each stage are given in Fig. 10. Except for the stage 0 curve, these are nearly constant for each stage where the aerosol has sufficient size range to cover them fully. The stage 0 curve applies only to one particular aerosol, because this stage has no fixed upper limit.

The principal parameters derived from the calibration are in Table 3, which is used as follows. From corrected bacterial colony counts, the number-distribution curve can be drawn by plotting the d_{50} values for the appropriate particle density against the cumulative numbers on the stages below. The mass-distribution curve can be obtained from this in the conventional way. Volume on each stage is the product of the colony count and the volume obtained from the MVD, where the aerosol size range adequately covers the stage. This figure can be used to estimate total cells per stage from samples of sprayed suspensions when the total solids content and cell count of the suspension are known, and when there has been no loss of viability. A comparison with impinger samples can therefore be made. Good agreement has been obtained in many such tests.

With nonviable samples which can be estimated, say, chemically, mass-distribution curves can be plotted directly from the stage estimates and the d_{50} values. Alternatively, the MMD values of Table 3 can be plotted against the cumulative mass for the stages below plus half that on the stage. The circles and triangles in Fig.

10 compare these methods of plotting with the dotted curve, which is from the summated counts of the aerosol that gave the stage 0 curve.

DISCUSSION

Stages 3 and below in the Andersen sampler function in a very satisfactory manner and in accord with the previous work of Ranz and Wong (1952). There is almost no slippage of particles beyond their proper stage. Stages 1 and 2 are not satisfactory, and the modifications described and the calibration given enable most of the important aerosol parameters to be obtained from the colony counts. The sampler has other desirable features, such as simplicity and speed in use, and is robust.

It is recommended that workers with modified forms of any stage should test them for jet uniformity by the heavy-sample method, sprayed clouds of india ink sampled on milk-agar being particularly suitable. Also, the intake cone should be discarded where possible because it causes heavy loss of larger particles on the top sieve.

Attempts to extend the size discrimination further upwards beyond the present work meet with the difficulty of high internal loss, because large particles are unable to make the 360° turn to the next stage. All detectable wall loss in the Andersen sampler is found on the sieves near the jet entrances and on the internal dish walls just above the agar. In the present geometry, these losses are unimportant.

When sampling in a wind, the sampler should be laid on its side facing into the wind. One may speculate that the broad multi-hole suction area may be a reasonable alternative, at least up to 20 μ, to isokinetic sampling, which in any case cannot be usefully achieved in a natural wind.

The use of the Andersen sampler is of course by no means confined to bacterial aerosols. Its high stage capacity will often be very useful for obtaining bulk samples of any kind of airborne dust or fine spray. For microscopy, the deposition of the sample in a large number of small, equal spots, each of which can be scanned in a few fields, is particularly useful. The impaction of particles is gentle, and there is no risk of particle or droplet shatter.

ACKNOWLEDGMENTS

It is a pleasure to thank C. O. Swenson for making many experimental models with great skill, W. N. Mott for much of the microscopical work, and many other members of the Physical Sciences Division, Fort Detrick, for expert assistance.

LITERATURE CITED

ANDERSEN, A. A. 1958. New sampler for the collection, sizing, and enumeration of viable airborne particles. J. Bacteriol. **76**:471–484.

MAY, K. R. 1945. The cascade impactor: an instrument for sampling coarse aerosols. J. Sci. Instr. **22**:187–195.

MERCER, T. T. 1963. On the calibration of cascade impactors. Ann. Occup. Hyg. **6**:1–14.

RANZ, W. E., AND J. B. WONG. 1952. Jet impactors for determining the particle size distribution of aerosols. Arch. Ind. Hyg. Occup. Med. **5**:464–477.